31st Int. Linear Accel. Conf. LINAC2022, Liverpool, UK JACoW Publishing
ISBN: 978-3-95450-215-8 ISSN: 2226-0366 doi:10.18429/JACoW-LINAC2022-TUPOPA09

RF MEASUREMENTS AND TUNING OF THE CERN 750 MHz ELISA-RFQ FOR PUBLIC EXHIBITION

M. Marchi,*,[1] H. W. Pommerenke,† A. Grudiev, S. Mathot, CERN, Geneva, Switzerland
[1]also at La Sapienza University of Rome, Italy

Abstract

Over the last few years, CERN has successfully designed, built, and commissioned the smallest RFQ to date, the one meter long PIXE-RFQ operating at 750 MHz. Its compactness offers a unique opportunity for education and public presentation of the accelerator community: A duplicate machine called ELISA-RFQ (Experimental Linac for Surface Analysis) will be exhibited in the Science Gateway, CERN's upcoming scientific education and outreach center. It will allow the public to approach within a few centimeters a live proton beam injected into air, which is visible to the naked eye. The construction of the ELISA-RFQ has been completed in 2022. In this paper, we present the results of low-power RF measurements as well as field and frequency tuning.

INTRODUCTION

The 750 MHz ELISA-RFQ, constructed at CERN, is a compact 1-meter long four-vane RFQ, an identical copy of the previous project PIXE-RFQ [1–4]. The small standalone RFQ will accelerate protons to 2 MeV and will be exhibited in the CERN's scientific education and outreach center, Science Gateway. There the audience will observe a live proton beam in air, visible to the naked eye. The RFQ key parameters are listed in Table 1.

The RFQ is subject to manufacturing imperfections and misalignments which lead to variations of the capacitance and inductance distribution. Therefore, the ideal quadrupole field of the TE_{210} operating mode is perturbed [5], and tuning of field and frequency is required. For ELISA-RFQ, the tuning algorithm developed for the HF-RFQ [6] based on Ref. [5] and improved for PIXE-RFQ [4] has been used.

SINGLE MODULE MEASUREMENTS

The ELISA-RFQ consists of two mechanical modules, brazed individually and then clamped together to form the full assembly. For each construction step, the vane positions were measured with respect to the ideal beam axis. The displacements after the final brazing step were within ±10 µm for the first module and ±17 µm for the second module.

Bead-pull measurements were performed on both the single modules to assess manufacturing quality. Very close agreement was observed by comparing measured resonance frequency and field profile to the simulation (eigenmode solver of CST Microwave Studio® 2020 [7]), thus no special measures were needed. Figs. 1a and 1b report the spectra of the two modules. Each was measured by placing two aluminum extension tubes at the upstream and downstream ends to have boundary conditions that can be reproduced in a 3D eigenmode simulation. For the quadrupole mode the observed deviations between the measured and simulated frequencies amount to 700 kHz for module 1 and less than 100 kHz for module 2. Fig. 2 shows the field components profiles of the single modules, where the dipole components show small deviations from the ideal zero simulation value (±3 %), whereas the quadrupole component has a deviation of less than ±1 % for both modules.

Table 1: Key Parameters of the ELISA-RFQ

Species	Proton	(H^+)
Input energy	20	keV
Output energy	2	MeV
RF frequency	749.480	MHz
Inter-vane voltage	35	kV
RFQ length	1072.938	mm
Vane tip transverse radius	1.439	mm
Mid-cell aperture	1.439	mm
Minimum aperture	0.706	mm
Final synchronous phase	−15	deg
Output beam diameter	0.5	mm
Beam transmission	30	%
Unloaded quality factor (Q_0)	6000	
Peak RF power loss	65	kW

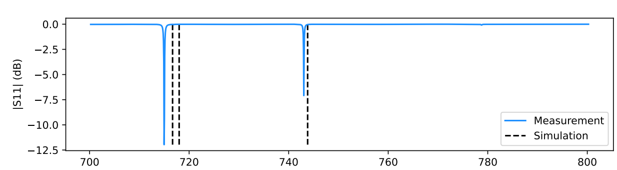

(a) Module 1

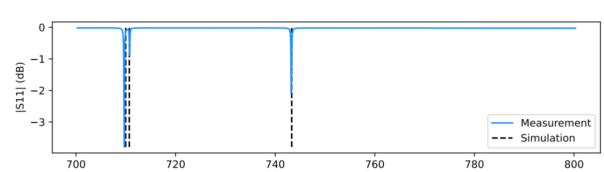

(b) Module 2

Figure 1: Measured reflection coefficient vs frequency for the single modules.

* mariangela.marchi@cern.ch
† hermann.winrich.pommerenke@cern.ch

ISBN: 978-3-95450-215-8 ISSN: 2226-0366 doi:10.18429/JACoW-LINAC2022-TUPOPA09

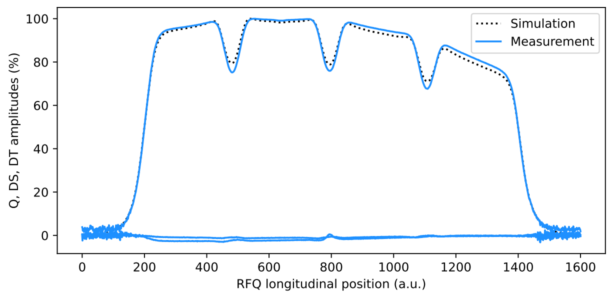

(a) Module 1

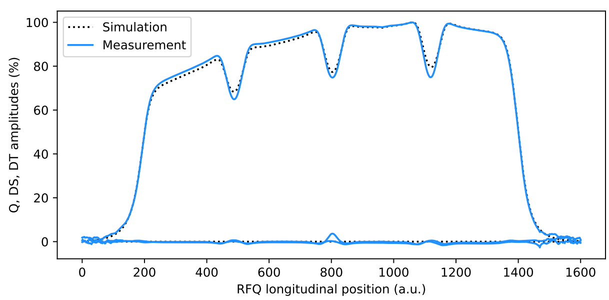

(b) Module 2

Figure 2: Measured quadrupole component Q and dipole components D^S, D^T of the single modules compared to the simulation.

TUNING

After the assembly, the ELISA-RFQ was tuned by means of sixteen movable copper piston tuners. The final length of each tuner was obtained by means of an iterative algorithm and bead-pull measurements carried out measuring the reflection $\Gamma \equiv S_{11}$ at the input power coupler. The goal of the tuning process is to achieve the target operating frequency of 749.480 MHz at 23 °C under vacuum, as well as a longitudinally constant ("flat") field distribution for the quadrupole component (Q) and ideally zero dipole components (D^S, D^T). Errors smaller than ±60 kHz and ±2 %, respectively, are acceptable. In this section, the steps of the tuning procedure and final tuner installation are reported. Field and frequency values before and after tuning are compared and discussed.

Tuning Setup and Algorithm

Fig. 3 shows the full assembly of the RFQ which includes the two modules, pumping ports, the RF input power coupler, four diagnostic antennas, and the two end plates.

The tuners were mounted in guidance tubes, attached to the outer surface of the tuning port flanges so that they can slide inside them and be carefully placed in the positions assigned by the algorithm iterations. The initial tuner position corresponds to the ideal insertion obtained from simulations [3]. The tuners are machined with an over-length of 11 mm to enable enabling a mechanical tuning range of ±11 mm. Thus, the initial position is 11 mm outward with

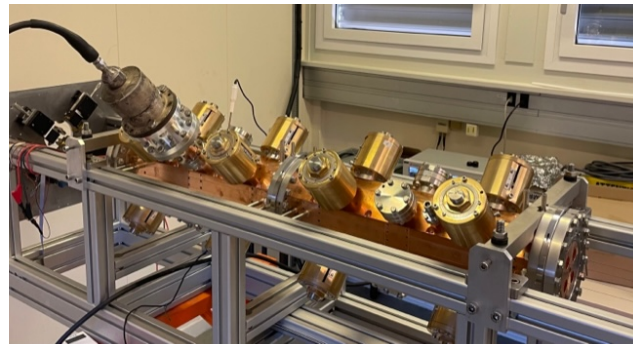

Figure 3: Photograph of the full assembly of ELISA-RFQ.

respect to the flange-to-flange position. Once the final positions are determined, the tuners are cut to their final lengths and installed flange-to-flange with copper gaskets. The tooling was originally developed for the HF-RFQ [6].

The augmented algorithm allows for tuning of field and frequency at the same time and is based on a response matrix description. The matrix **R** represents the Jacobian of the field amplitudes (three components at 8 discrete locations) and frequency values with respect to the tuner positions. At each tuning step, the new corrective tuner positions are obtained as

$$t_{\text{trg}} = t_{\text{cur}} + \mathbf{R}^{\dagger}\Delta x, \tag{1}$$

where t_{trg} and t_{cur} are target and current tuner position vectors, respectively, Δx is the difference between target and current field amplitudes and frequency and $\mathbf{R}^{\dagger}$ denotes the Moore-Penrose inverse [8] of **R**. The inverse was computed using the method based on singular value decomposition (SVD) [8] proposed in Ref. [6] and used also in Ref. [4].

Tuning Steps

The entries of **R** were determined by retracting individually the tuners by 3 mm and performing spectrum and bead-pull measurements for each tuner. Fig. 4a is a visual representation of the response matrix in which only the field sensitivities are shown. Fig. 4b reports the frequency sensitivities.

The ELISA-RFQ was tuned in four steps after the measurement of **R**: the first two were given by the algorithm whereas the last two were manual adjustments to fine-tune the frequency (all tuners moved by the same amount). It was decided to move the tuners by half of the adjustments proposed by the algorithm at step 1 and 2 of tuning since an overshooting had been observed. This likely originated in the non-linearity of the problem and that the quadrupole error was close to the measurement noise level already before tuning. (Overshooting was not observed on the PIXE-RFQ [4].) The errors in field components and frequencies are reported in Table 2 for each tuning step. After the second step, the errors in the field components fulfilled the requirements. Fig. 5 shows the field for each tuning iteration.

ISBN: 978-3-95450-215-8 ISSN: 2226-0366 doi:10.18429/JACoW-LINAC2022-TUPOPA09

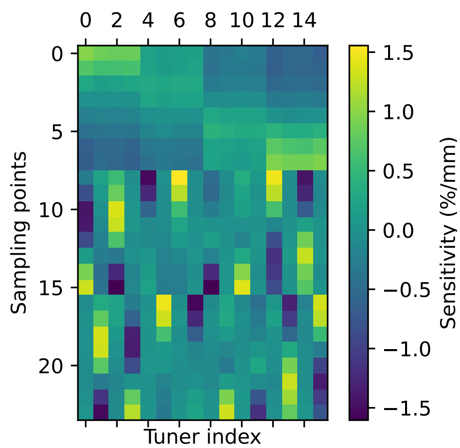

(a)

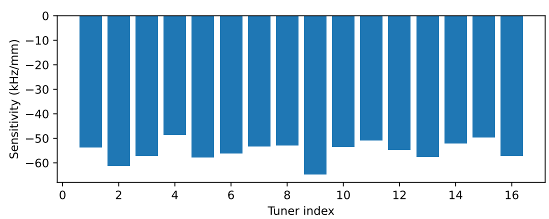

(b)

Figure 4: (a) Visual representation of **R** in which the entries represent Q, D^S, D^T sensitivities at one sampling point for each tuner movement. (b) Responses of operating mode frequency for each tuner movement.

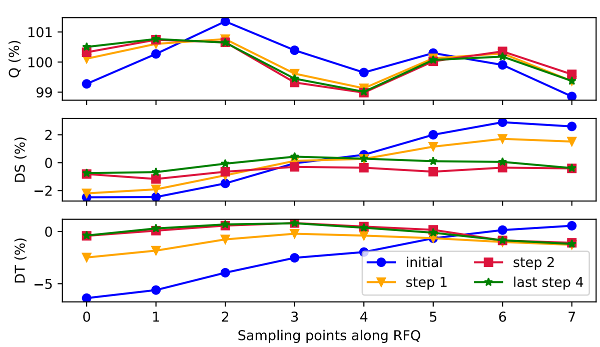

Figure 5: Measured field components for the initial tuner configurations and for each tuning step.

QUALITY FACTOR MEASUREMENT

To validate the design of ELISA-RFQ the quality factors were also measured. After tuning, the complex reflection coefficient Γ was measured in a bandwidth of 2 MHz around the operating frequency. Unloaded (Q_0), external (Q_{ex}), loaded (Q_ℓ) quality factors and the coupling coefficient (β_c) could be obtained by fitting an ideal circle to Γ following the method described in Refs. [9–12]. In Table 3 measured quality factors and coupling coefficient are compared to the design values.

Table 2: Errors in field components and frequency for tuning steps in chronological order.

Step	δQ (%)	δD^S (%)	δD^T (%)	Δf (kHz)
Initial	1.35	2.89	6.38	224.56
Step 1	0.87	1.91	2.49	134.31
Step 2	1.02	1.17	1.08	62.94
Step 3	—	—	—	-47.47
Step 4	0.99	0.75	1.19	-1.50

Table 3: Quality factors and coupling coefficient obtained through the circle-fitting method and their design values.

	Measured	Design	Rel. Error (%)
Q_0	6039	5995	0.7
Q_{ex}	4977	4796	3.8
Q_l	2728	2664	2.4
β_c	1.21	1.25	3.2

CONCLUSION

In this paper, we have reported the low-power RF measurements and tuning of the 750 MHz ELISA-RFQ. Bead-pull measurements on individual mechanical modules have shown the high manufacturing quality of the RFQ. The remaining field and frequency errors have been successfully corrected using an iterative tuning procedure, with final values well within target ranges. Moreover, excellent agreement was observed in quality factors and coupling.

Additional bead-pull measurements will be carried out following the cutting of the tuners to confirm the field profile. After the tuners have been installed with copper gaskets, further RF measurements will confirm the operating frequency under vacuum. The ELISA-RFQ is expected to commence operation at Science Gateway at CERN in 2023.

REFERENCES

[1] M. Vretenar *et al.*, "High-frequency compact RFQs for medical and industrial applications," in *28th Linear Accelerator Conference (LINAC2016), East Lansing, MI, USA*, 2016, pp. 704–709, doi:10.18429/JACoW-LINAC2016-TH1A06

[2] A. Lombardi, M. Vretenar, S. Mathot, and A. Grudiev, "High frequency compact low-energy linear accelerator design," US Patent 10,051,721, Current assignee: CERN (European Organization for Nuclear Research), 2018.

[3] H. W. Pommerenke *et al.*, "RF design studies on the 750 MHz radio frequency quadrupole linac for proton-induced x-ray emission analysis," *Phys. Rev. Accel. Beams*, vol. 22, no. 5, 2019, doi:10.1103/physrevaccelbeams.22.052003

[4] H. W. Pommerenke, U. van Rienen, and A. Grudiev, "RF measurements and tuning of the 1-m-long 750 MHz radio-frequency quadrupole for artwork analysis," *Nucl. Instrum. Methods Phys. Res., Sect. A*, vol. 1011, p. 165 564, 2021, doi:10.1016/j.nima.2021.165564

ISBN: 978-3-95450-215-8 ISSN: 2226-0366 doi:10.18429/JACoW-LINAC2022-TUPOPA09

[5] T. P. Wangler, *RF Linear Accelerators*, 2nd ed. John Wiley & Sons, 2008, doi:10.1002/9783527623426

[6] B. Koubek, A. Grudiev, and M. Timmins, "RF measurements and tuning of the 750 MHz radio frequency quadrupole," *Phys. Rev. Accel. Beams*, vol. 20, no. 8, 2017, doi:10.1103/physrevaccelbeams.20.080102

[7] Computer Simulation Technology, *CST Studio Suite®, release 2018*, 2018.

[8] I. N. Bronshtein, K. A. Semendyayev, G. Musiol, and H. Mühlig, *Handbook of Mathematics*. Springer Berlin Heidelberg, 2015, doi:10.1007/978-3-662-46221-8

[9] W. Altar, "Q circles-a means of analysis of resonant microwave systems," *Proceedings of the IRE*, vol. 35, no. 5, pp. 478–484, 1947, doi:10.1109/jrproc.1947.232938

[10] D. Kajfez, "Linear fractional curve fitting for measurement of high q factors," *IEEE Transactions on Microwave Theory and Techniques*, vol. 42, no. 7, pp. 1149–1153, 1994, doi:10.1109/22.299749

[11] D. Kajfez, "Random and systematic uncertainties of reflection-type Q-factor measurement with network analyzer," *IEEE Transactions on Microwave Theory and Techniques*, vol. 51, no. 2, pp. 512–519, 2003, doi:10.1109/tmtt.2002.807831

[12] V. A. Goryashko *et al.*, "High-precision measurements of the quality factor of superconducting cavities at the FREIA laboratory," in *17th International Conference on RF Superconductivity (SRF2015)*, 2015, pp. 810–813, doi:10.18429/JACoW-SRF2015-TUPB083